

Investigation of MCCI Phenomena with Multi-Physics MPS Simulation

Penghui Chai¹, Nedjet Erkan¹, Masahiro Kondo¹ and Koji Okamoto¹

¹: Department of Nuclear Engineering and Management, University of Tokyo, Hongo 7-3-1, Bunkyo ku, Tokyo, 113-8654, Japan
phchai@vis.t.u-tokyo.co.jp

Abstract

Molten core concrete interaction (MCCI) phenomenon is investigated with a developed code based on moving particle semi-implicit (MPS) method. Momentum and energy equations are solved to resolve the velocity field and temperature field respectively. Various models are developed to simulate the mechanisms existing in the MCCI such as heat transfer model, phase change model, mixing model, chemical reaction model, and gas generation model. A visualization experiment was conducted in order to validate the heat transfer model and phase change model. U-alloy and transparent gel wax, which have similar density ratio as MCCI, were selected as the materials used in the experiment. Interaction of two materials, ablation and solidification was observed very clearly. Spreading characteristic of molten metal alloy is captured and quantified. Those quantities include final shape of solidified metal, time resolved motion of melt, ablation speed, and related temperatures. Good agreement can be observed between the simulation and the experiment on both temperature and ablation behavior. This consistency suggests that enhanced MPS method can simulate such erosion process appropriately. Additionally, an experiment in the literature utilizing Tin as a working fluid is simulated to validate the natural circulation model. The results show a good agreement on both temperature distribution and velocity field. CCI experiment is simulated by assemble all the models. The decay heat for each dehydration reaction is predicted. The result shows the similar trend as the experiment and suggests that the chemical reaction and gas generation may play a very important role to precisely simulate the ablation behavior.

Keywords:

MCCI, MPS method, CFD, Phase change.

1 Introduction

Molten Core-Concrete Interaction (MCCI) is supposed to take place after the early pressure vessel failure. The corium will melt through the pressure vessel and discharge into the reactor cavity and erode the concrete basemat if the emergency measurement failed during the core melt accident. There are two main mitigation measurements in most of the current nuclear reactor. One is flooding it after the melt discharged the dry vessel cavity while another one is filling the vessel cavity before the failure of pressure vessel. However, even if the mitigation measurements work normally, the melt might result in catastrophic large fission product release and the land contamination due to the containment failure because of the pressurization based on the large gas generation during the Corium-Concrete Interaction and the melt-through of the basemat. Therefore the gas generation behavior and the ablation behavior in MCCI are to be studied.

To work out this issue, extensive experiment researches have been carried out since 1980s. Such as Beta series [1], ACE series [2], SURC series [3-6], WETCOR series [7], MACE series [8], CCI series [9, 10] et al. The main objective of these large-scale experiments is to investigate the ablation behavior, chemical reaction between corium and concrete and the gas generation during the MCCI process. Different corium and concrete composition were utilized in the experiments to figure out the effect of parametric variations on the phenomena. Most of the experiment got the results what they expected. The gas release evidence and the 1D ablation behavior were major finding of the experiments before 1990s, and recent experiments are mainly focusing on the 2D aspect of the

ablation with considering the axial versus radial erosion and the role of crust formation during the process. The major finding of these experiment is the evidence that the lateral erosion plays a very important role during the ablation process[9, 10], which suggests the necessity of 2D ablation behavior research.

Besides, several numerical simulation studies were also applied by previous researchers, such as ASTEC/MEDICIS, WECHSL, MELCORE, et al [11-15]. Since various physical and chemical phenomena are to be considered in MCCI process, various calculation models were proposed in the codes. Different heat transfer correlations between concrete and corium were applied, as well as the interface model on the crust area and concrete ablation model. Although most of the codes were validated against the experiments, it showed the big deviation in predicting the ablation shape of the corium and the temperature of the melt based on the different interfacial models in different codes[12]. Thus, it suggests the limitation of the empirical formula application in the MCCI simulation, and indicates the necessity to develop a code in which only fundamental governing equations are used in order to mechanically understand the interaction phenomena.

For this purpose, some researchers simulated the previous MCCI experiments using Moving Particle Semi-implicit (MPS) method. MPS method [16-19] is one of the particle methods based on the Lagrangian description, which initially developed by S.Koshizuka and Oka in 1990s. The most important merit of MPS method in investigating MCCI process is that large deformation of interfaces can be analyzed without grid tangling and numerical diffusion since the convection terms are directly calculated by the motion of the particles. Numerous research with complex motion of free surfaces were successfully analyzed by the MPS method, such as the collapse of water column[20] and wave breaking[21]. Therefore, MPS method is utilized as a tool to analyze the mechanistic of phenomena in MCCI process. SWISS-2 experiment was simulated by S.Koshizuka[22] in 2001, in which heat transfer model and phase-change model were developed to simulate the ablation phenomenon. The study concluded that mechanistic analyses based on fundamental governing equations without empirical correlations were useful to understand the phenomena in detail. However, the calculated ablation speed of concrete was slower than that of the experiment. Besides, it did not conserve total mass and energy because it adopted the simplistic phase change model in which the concrete particles were directly changed to the corium particles when they exceeded the melting temperature. SURC-2 experiment was calculated by X.Li[23]. Results showed the good agreement with the experiment and they concluded the chemical reaction of Zirconium is sensitive to the simulation results. However, similar to the research by S.Koshizuka in 2001, the simplified phase change model was used in this simulation, which made the concrete particles immiscible with the corium. Besides the disadvantage on mixing part, both of them select one dimensional experiment to validate the code, which means the lateral ablation process is ignored in the simulation. But based on the recent experiment results, lateral ablation show more efficient than that in axial direction. Thus, it suggests the further development of MPS code and related validation work is necessary for MCCI simulation.

However, the experiments for the validation of models addressing several MCCI relevant physical phenomena are very rare in the literature. Especially, details of the ablation process is never been visualized because of the extreme experiment conditions. Therefore, a visualization experiment is necessary to observe the details of ablation and melt progression for the validation.

In this paper, a new computation code is developed based on MPS method to simulate MCCI phenomena. The heat transfer model, phase-change model, natural circulation model, surface tension model, chemical reaction model and gas generation model are implemented. Additionally a small-scale validation experiment is conducted. A metallic alloy with low melting temperature is employed to reproduce the molten corium behavior at low temperature conditions. Gel wax is chosen to be ablated not only because of its transparent properties, but also because of the density ratio between the wax and U-alloy is similar to the ratio of corium and concrete in the real MCCI case. The developed code is applied to simulate this experiment and the results were compared to validate the models. Besides wax experiment, CCI-2 experiment, a two-dimensional MCCI experiment with lateral ablation process, is selected to validate the developed code.

2 Numerical methodBasic MPS method

The governing equations of MPS method are the continuity equation, the Navier-Stokes equation and Energy conservation equation:

$$\nabla \cdot \mathbf{u} = 0 \quad (1)$$

$$\frac{\partial \mathbf{u}}{\partial t} + (\mathbf{u} \cdot \nabla) \mathbf{u} = -\frac{1}{\rho} \nabla p + \nu \nabla^2 \mathbf{u} + \mathbf{F} \quad (2)$$

$$\frac{\partial h}{\partial t} = k \nabla^2 T + Q \quad (3)$$

where ρ , t , \mathbf{u} , p , ν , \mathbf{F} , h , k , T and Q are density, time, velocity vector, pressure, kinematic viscosity, external force, enthalpy, thermal conductivity, temperature and heat source, respectively.

In the MPS method, the fluid is represented by moving particles. The particle interaction is defined within a constant distance r_e by using a kernel function $w(r)$:

$$w(r) = \begin{cases} \frac{r_e}{r} - 1 & (r < r_e) \\ 0 & (r \geq r_e) \end{cases} \quad (4)$$

where r is the distance between two particles i and j .

The parameter n_i is a particle number density for particle i , which is defined as

$$n_i = \sum_{j \neq i} w(|\mathbf{r}_j - \mathbf{r}_i|) \quad (5)$$

where \mathbf{r}_j and \mathbf{r}_i is the coordinate of particle i and j . It represents the density of particles around particle i . In the case of incompressible fluid, the particle number density of fluid is kept constant. The continuity equation is satisfied automatically by holding the total number of particles and the mass of individual particles constant.

The gradient of the scalar field ϕ at particle i is computed by the weighted average of gradient vectors as

$$\langle \nabla \phi \rangle_i = \frac{d}{n^0} \sum_{j \neq i} \left[\frac{\phi_j - \phi_i}{|\mathbf{r}_j - \mathbf{r}_i|^2} (\mathbf{r}_j - \mathbf{r}_i) w(|\mathbf{r}_j - \mathbf{r}_i|) \right] \quad (6)$$

where d is the space dimensions number.

In the MPS method, the Laplacian of ϕ is discretized by distributing a part of ϕ from particle i to its neighbor particles using the kernel function as

$$\langle \nabla^2 \phi \rangle_i = \frac{2d}{n^0 \lambda} \sum_{j \neq i} [(\phi_j - \phi_i) w(|\mathbf{r}_j - \mathbf{r}_i|)] \quad (7),$$

where λ is a parameter which is chosen so that the variance fits the analytical value.

$$\lambda = \frac{\int_V w(r) r^2 dv}{\int_V w(r) dv} \quad (8)$$

A semi-implicit algorithm is employed in the MPS method. Viscosity term and external force terms in the Navier-Stokes equation are explicitly calculated in order to obtain the temporary velocities \mathbf{v}_i^* , and the temporary coordinates \mathbf{r}_i^* , $\mathbf{v}_i^{(k)}$ and $\mathbf{r}_i^{(k)}$ the velocity and coordinate from the last time step, the particles are moved based on the following equation.

$$\mathbf{v}_i^* = \mathbf{v}_i^{(k)} + \Delta t (\nu \nabla^2 \mathbf{v}_i^{(k)} + \mathbf{g}) \quad (9)$$

$$\mathbf{r}_i^* = \mathbf{r}_i^{(k)} + \mathbf{v}_i^* \Delta t \quad (10)$$

where Δt is the time-step width, and subscripts on the right shoulder k shows the time step, and \mathbf{g} is the vector of gravity. The pressure is then calculated by solving the Poisson Equation as

$$\langle \nabla^2 P \rangle_i = -\frac{\rho}{\Delta t^2} \frac{n_i^* - n^0}{n^0} \quad (11)$$

By solving this equation, corrected velocity is obtained. Corrected convection is calculated by the corrected velocity, and particle i is going to move to its final position of this time step.

$$\mathbf{v}_i^{k+1} = \mathbf{v}_i^* - \frac{\Delta t}{\rho} \cdot \nabla P \quad (12)$$

$$\mathbf{r}_i^{(k+1)} = \mathbf{r}_i^* - \frac{\Delta t^2}{\rho} \nabla P \quad (13)$$

More detail explanation of MPS method can be found in the references[20, 21].

2.2 Heat transfer and phase-change model

Heat transfer between particles is discretized based on the energy equation (Eq.3). The equation can be explicitly solved by using Laplacian model:

$$\frac{Dh_i}{Dt} = \frac{2d}{n^0 \lambda} \sum_{j \neq i} \left[k_{ij} (T_j - T_i) w(|\mathbf{r}_j - \mathbf{r}_i|) \right] + Q_i \quad (14)$$

Where h and Q are the enthalpy and heat source of particle i , respectively. Temperature will then be calculated by enthalpy h . To calculate the temperature during the phase change, the melting temperature T_s , the solid enthalpy at the melting point h_s and liquid enthalpy at the melting point h_l are used.

The temperature is calculated by Eq.15, where T_s and T_l is solidus temperature and liquidus temperature respectively.

$$T = \begin{cases} T_s + \frac{h - h_s}{\rho C_{ps}} & (h < h_s) \\ T_s + \frac{h - h_s}{h_l - h_s} (T_l - T_s) & (h_s \leq h \leq h_l) \\ T_l + \frac{h - h_s}{\rho C_{pl}} & (h_l < h) \end{cases} \quad (15).$$

For the material which has fixed melting point, the solidus and liquidus temperature will be set as same as the melting temperature, like Eq.16 shows.

$$T_s = T_l = T_{melt} \quad (16)$$

To express the phase change, solid-fraction γ is introduced and calculated based on the enthalpy h by

$$\gamma = \begin{cases} 1 & (h < h_s) \\ \frac{h_l - h}{h_l - h_s} & (h_s \leq h \leq h_l) \\ 0 & (h_l < h) \end{cases} \quad (17),$$

which is used as a criteria to judge the phase of the material.

2.3 Surface tension model

Surface tension model is essential since there are two immiscible materials at the melt pool in the simulation, and melt metal has a very high surface tension. In this study the model developed by M.Kondo[24] in 2006 is adopted. In this model, surface tension is represented by the potential force between the particles

$$\begin{cases} P(r) = \frac{C}{3} \left(r - \frac{3}{2} r_{\min} + \frac{1}{2} r_e \right) (r - r_e)^2 & (r \leq r_e) \\ P(r) = 0 & (r \geq r_e) \end{cases} \quad (18),$$

where r , r_{\min} , r_e and C are the particle distance, the initial minimum particle distance, the effective radius of the potential force and a fitting coefficient, respectively. The coefficient C controls the strength of surface tension. Surface tension is strong when C is large. In this study, $r_{\min}=d$, $r_e=3.1d$ is used. As shown in Figure.1, a unit area $S=r_{\min}^2$ between two fluid is established to simulate the surface energy inside it. To create this area, the particles existing from area A should be detached from the particles existing from area B. This is shown in Eq.19. Combine the Eq.18, C can be derived as Eq.20

$$2\sigma r_{\min}^2 = \sum_{i \in A, j \in B} P(r_{ij}) \quad (19)$$

$$C = \frac{3 \times 2\sigma r_{\min}^2}{\sum_{i \in A, j \in B, |r_{ij}| < r_e} (r_{ij} - \frac{3}{2}r_{\min} + \frac{1}{2}r_e)(r_{ij} - r_e)^2} \quad (20)$$

where σ is the surface tension coefficient of the material. This is the relationship between the potential force and surface tension. Particles convection can be subsequently calculated by the Eq. 21.

$$m \frac{d\vec{v}}{dt} = C(r_{ij} - r_{\min})(r_{ij} - r_e)\vec{n}_{ij} \quad (21)$$

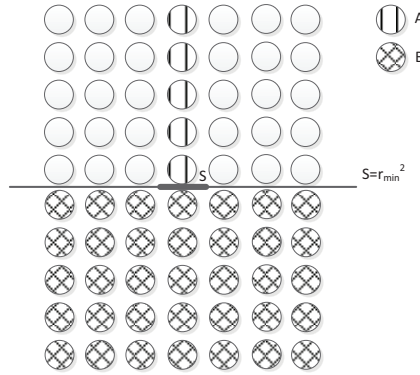


Figure 1. Surface energy estimation.

2.4 Mixing model

As discussed in the introduction part, previous MCCI simulation by using MPS method didn't arrange good when the concrete mixed into the corium pool. Thus, a new mixing model is essential to conserve the total mass and total energy during the calculation.

The melt properties will be changed when the concrete eroded into the corium.

$$\varphi_{melt} = \frac{\varphi_{corium} \times (N_{corium} - N_{crust}) + \varphi_{concrete} \times N_{melt}}{N_{corium} - N_{crust} + N_{melt}} \quad (22)$$

Where φ_{melt} , φ_{corium} , $\varphi_{concrete}$ is the properties of current melt pool, initial corium and concrete respectively. N_{corium} , N_{crust} , N_{melt} is the total particle amount of initial corium, current crust and melted concrete respectively. This equation means when the concrete particle touch the corium particles, it will be switch to corium particle type. Meanwhile, the new properties of the melt pool will be recalculated by the composition of corium and concrete. In particular, the material properties is going to be averaged after the concrete mixed. So that the total mass and total energy are conserved during the simulation.

3 Wax experimental setup and simulation conditions

3.1 Experimental setup

In order to validate the CFD simulation, dynamic ablation behavior data is necessary for the comparison. However, it's almost impossible to visualize in the large-scale MCCI experiments because of the extreme experimental conditions. Besides, the setting of the experiment to test the ablation of concrete in a MCCI event is costly and need high-level safety procedures. Therefore, a simple alternative experiment at low temperatures using u-alloy and transparent materials has been performed to emulate the ablation behavior in MCCI. It allows us

to obtain more quantitative data with ease by the visualization and temperature measurements. U-alloy and gel wax were selected to emulate the corium and concrete in the MCCI process, respectively. Their density ratio between u-alloy and gel wax is 2.70, and it is close to the ratio between corium and concrete which is 3.42.

The gel wax was filled in a transparent glass container with 7cm×7cm×6cm size. Unlike the large scale MCCI experiment, the experiment proceeded under pure dry cavity conditions. Initially u-alloy was heated up in the hot pot until 190°C, while the temperature of gel wax was 20°C. Then, melted u-alloy was poured into the cylindrical cavity at the central of the pool made of gel wax. Ablation was immediately started right after the pouring. Ablation movement was captured by high speed camera in a frequency of 2fps. Temperature was measured with three K-type thermal-couples at the locations of (-1.0cm, 0.5cm), (-1.0cm, 1.8cm) and (0cm, 3.5cm). The data acquisition was done by a data logging system whose frequency is 1fps.

3.2. Simulation configuration

A 2-dimensional domain is established to simulate the experiment by MPS method as shown in Figure.2. There are three types of particles, represented by blue, green and red in Figure.2. They are u-alloy particles, gel-wax particles and wall particles, respectively. The representing material does not change through the calculation and it ensures the conservation of mass and heat. The wall particles are only used to calculate the particle number densities. Since they do not exchange heat with the inner particles, the wall was modeled adiabatic in this simulation. To express the phase change of the gel-wax, each gel-wax particle is judged whether it is fluid or solid using Eq.16 in every time step. The fluid particles' movement is calculated by solving the momentum equation, while the solid particles are fixed to the previous position. The initial simulation condition is shown in Table 1, and the material properties [25-27] used in the code are shown in Table 2.

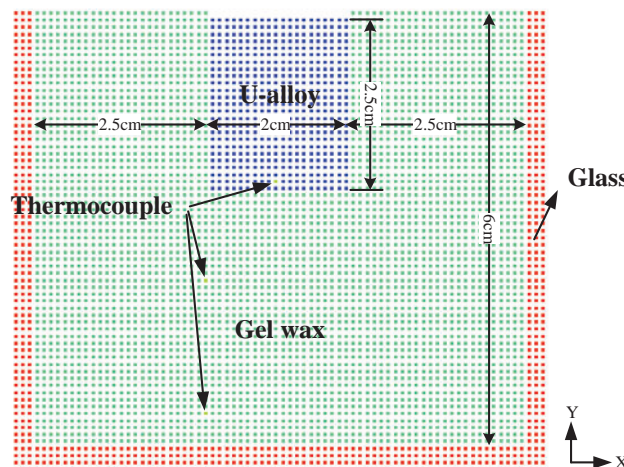


Figure 2. Initial particle configuration

Table 1. Initial condition of the simulation

Parameter	Value
Initial temperature of gel wax (K)	293.0
Initial temperature of u-alloy (K)	464.0
Average distance between particles (m)	0.001
Total number of particles	9126

Table 2. Physical properties of materials

Properties	U-alloy	Gel wax	Glass
------------	---------	---------	-------

Density(g / m^3)	9580.0	3550.0	2300.0
Thermal conductivity($W / m \cdot K$)	36.0	0.4	1.09
Specific heat($J / (kg \cdot ^\circ C)$)	790.0	780.0	600.0
Latent heat(J / kg)	45800.0	43700.0	-
Melting point($^\circ C$)	70.0	50.0	2000.0

3.3 Results and discussion

The profile of metal deformation process can be seen in the pictures (Figure.3). The process could mainly be divided into 2 stages. From the very beginning to around 80s, ablation process is nearly homogenous due to the uniform temperature distribution of the melt pool. Besides that, crust was generated after around 60s in the bottom of the melt, which decreased the heat transfer between the molten metal and gel wax. The second stage is from 80s, molten metal gained its final shape after some time and continued its downward motion with preserving its shape. This is due to the heat sink effect from the gel, the surface temperature is decreased until solidification point of the u-alloy. Therefore, a shell was gradually generated and surrounded the melting material. However, ablation process did not stopped because the surface temperature was still higher than the melting point of gel wax. The final melting depth in the central line was 2.2cm.

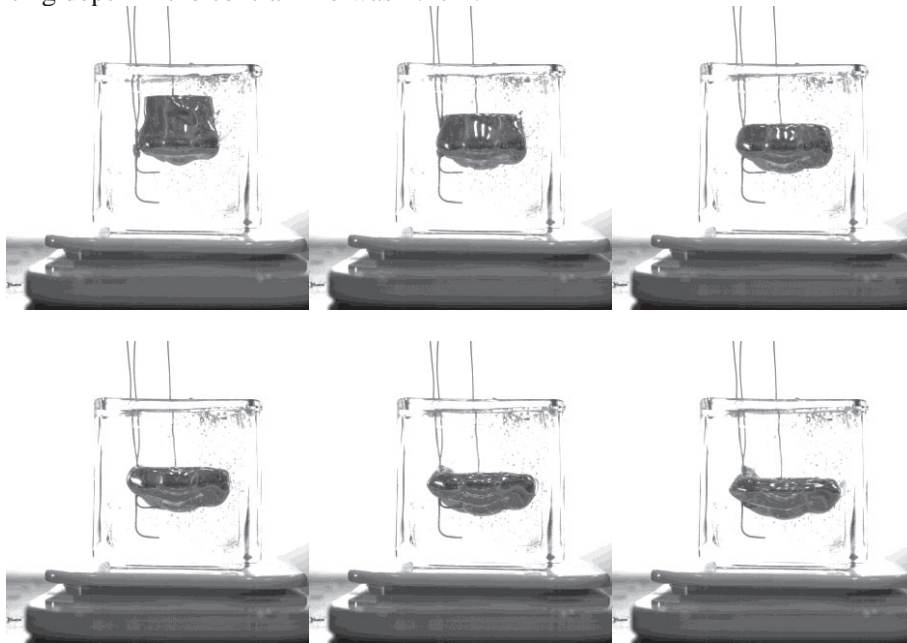


Figure 3. Ablation process and metal deformation along the elapse time. (First line, from left to right: 5s, 20s, 40s; Second line, from left to right: 60s, 80s, 100s.)

Figure.4 is a series of pictures to show the comparison of ablation profile between the simulation and the experiment at three time points. In order to clearly compare the molten metal deformation process with the experiment, the particles are represented by their material type. It is depicted from the pictures that the ablation profile simulated by MPS method agreed with the experiment.

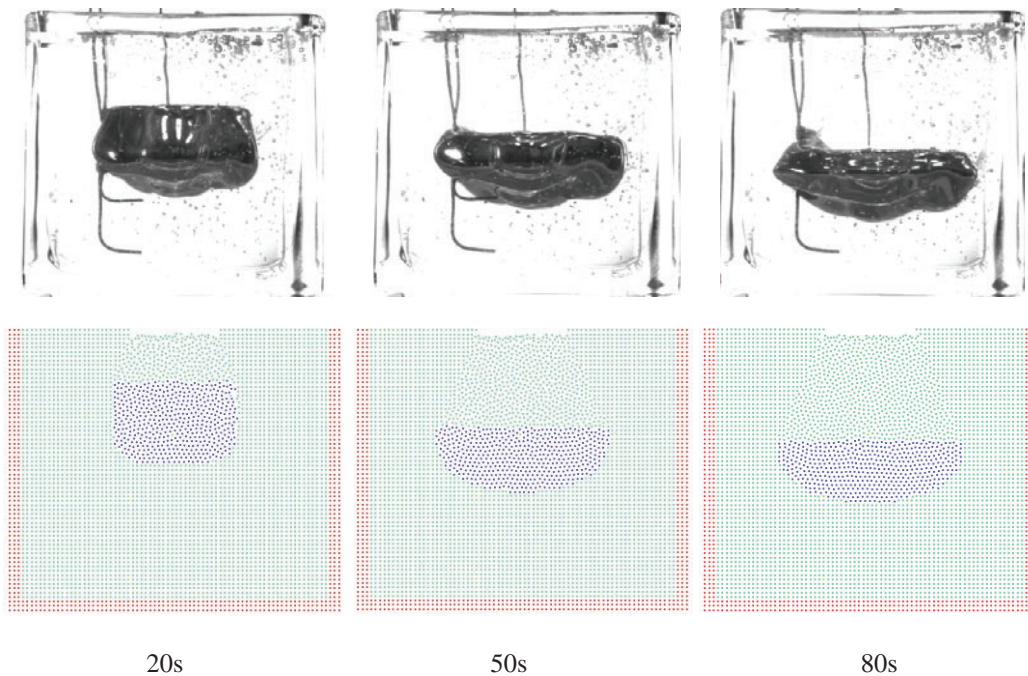


Figure 4. Ablation profile comparison between simulation and the experiment at 20s, 50s, 80s.

Figure.5 shows the comparison of erosion front head with both axial and radial direction between the experiment and MPS method. A good agreement on both downward and sideward ablation could be seen in the picture. The liquid metal melted the wax almost homogenously. The ratio of axial and lateral ablation at the end is 1.27, which is quiet similar to the experiment results. The ablation speed is gradually decreasing along the elapse time.

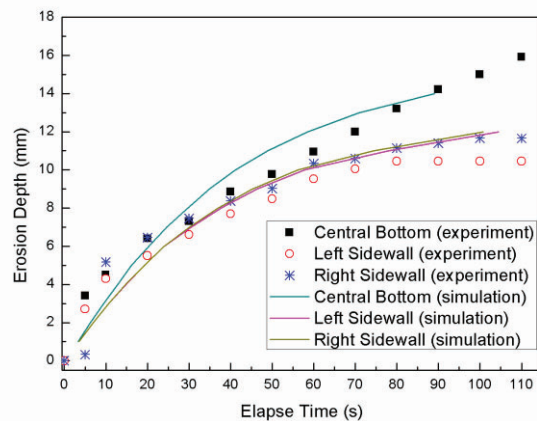


Figure 5. Erosion front head during the ablation process

Figure.6 is a series of pictures showing the temperature distribution of the whole region along the elapse time in the simulation. It can be seen from the pictures that the temperature of u-alloy decreased due to the heat sink effect from the gel wax. Besides, it appeared very small temperature diffusion due to the low thermal conductivity of gel wax.

All in all, it shows the heat transfer and phase change of moving molten pool can be emulated by this code, which suggests the possibility to be extend to the real MCCI calculation.

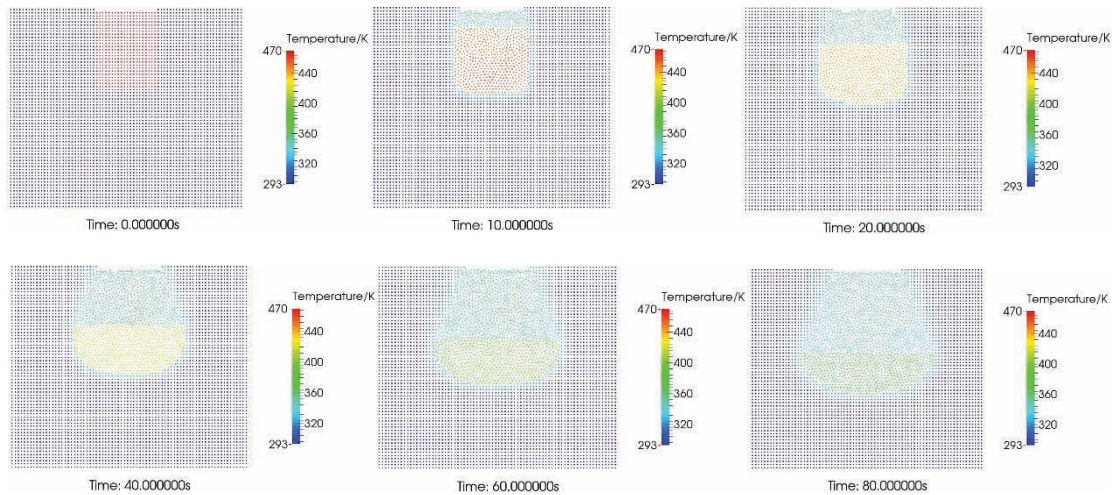


Figure 6. Temperature changes with elapse time

4 Natural circulation validation

A number of experiments and numerical simulation were conducted to investigate natural convection in the melt pool[28-30], which shows it is foundationally important to analyze the heat transfer inside the corium[31]. Verification work for MPS method was conducted [18], which shows MPS method can give excellent results for low and moderate Rayleigh number. However, some deteriorate exits in the high Rayleigh number condition, it shows the smaller temperature gradient than the analytical results. Therefore, to validate the natural circulation model, a pure natural convection experiment [32] is simulated.

4.1 Configuration

In the experiment [32], as shown in Figure.7, the tin was put into a rectangular cavity with two vertical side walls at constant but different temperatures. The remaining walls of the cavity were well insulated. The configuration of the simulation is depicted in Figure.7, which has the same initial condition as the experiment. The physical properties of tin and the initial condition of simulation are listed in Table 3 and Table 4, respectively.

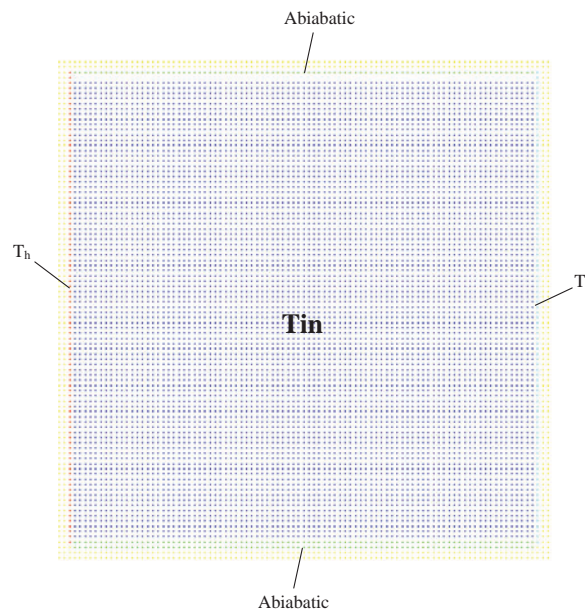


Figure 7. Configuration of the simulation.

Table 3. Physical properties of tin

Density (g / m^3)	Thermal conductivity ($W / m \cdot K$)	Specific heat ($J / (kg \cdot ^\circ C)$)	Dynamic viscosity ($N / m \cdot s^2$)	Melting point ($^\circ C$)	Thermal expansion coefficient ($10^{-6} / K$)
7310.0	66.0	210.0	0.00166	231.93	22

Table 4. Initial condition of the simulation

Parameter	Value
Initial tin's temperature(K)	506.2
Hot plate temperature T_h (K)	507.4
Cold plate temperature T_c (K)	505.0
Average distance between particles (m)	0.001
Total number of particles	9126

4.2 Results and discussions

Figure.8 shows the comparison of the isothermal contour of both experiment and MPS method simulation using non-dimensional value $\xi = x/L, \eta = y/H$. Similar trend on the temperature field was obtained. Figure.9 shows the comparison of the temperature history in three certain places among experiment, MPS method and FLUENT, which is a CFD code assembled in ANSYS software. In the figure, the results are shown using the non-dimensional value $\Theta = \frac{T-T_c}{T_h-T_c}$. We can see from the figure that both FLUENT and MPS method obtain the

reasonable results. However, difference between the experiment and simulation can be observed from the Figure.8 and Figure.9, especially at the location of top-right corner and bottom-left corner, where the big temperature gradient exists. This tendency is similar to the MPS calculation done by Shuai Zhang in 2005[18], the temperature gradient is smaller than that in the experiment. He calculated Nusselt number to estimate the magnitude of the error compared to the analytical results, which is about 11% when $Ra = 1 \times 10^5$ [18]. The Rayleigh Number in this study is about 3.625×10^5 , which is larger than the case in the verification study[18]. Therefore, the error in this study was also larger when compared to the tin experiment [32]. This supports the conclusion in the verification work[18]. That is to say, although the natural circulation can be excellent simulated by MPS method at the low Rayleigh number condition, but underestimated when the Rayleigh Number is going high. However, the Rayleigh number is not high for a pool calculation in the MCCI simulation, which suggests the code might be able to be extended to the real MCCI simulation.

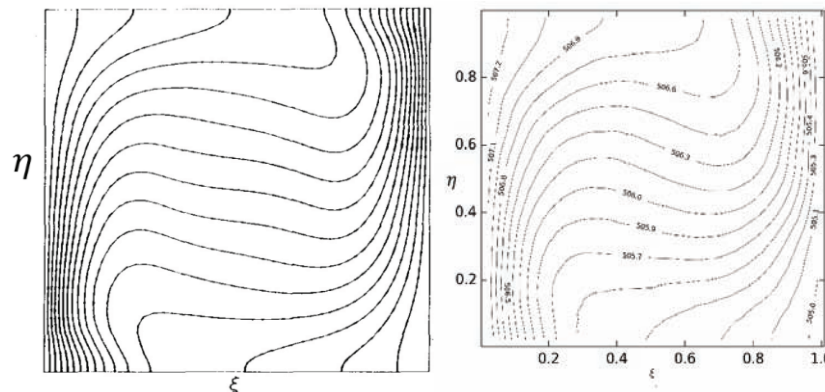


Figure 8. isothermal contour comparison of the experiment (Left) [32] and the simulation (Right).

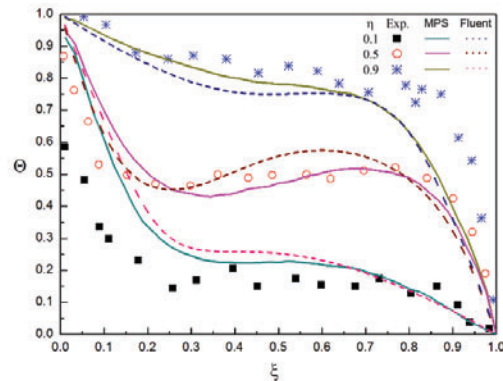


Figure 9. Comparison of temperature in three places between experiment, MPS method and Fluent

5 CCI-2 experiment simulation

5.1 CCI-2 experiment

CCI series experiments[33] are part of the OECD-MCCI program and performed from 2003. The objective of the experiments are resolve the ex-vessel debris cool ability issue by providing both confirmatory evidence and test data for cool ability mechanisms identified in previous integral effect tests, and address remaining uncertainties related to long-term 2-D core-concrete interaction under both wet and dry cavity conditions. The reasons why CCI-2 experiment was selected to be analyzed are following 3 parts.

- 1) CCI-2 experiment is a 2-dimensional MCCI experiment with lateral concrete ablation, which is not considered in the previous MPS simulation.
- 2) CCI-2 experiment is performed initially in dry condition and the initial melt compositions were predominately oxides. Although the data from the test may not be applicable for the real nuclear plants, but the results are useful for code validation purposes.
- 3) CCI-2 experiment use limestone type concrete, which is convenient to analyze the how the gas generation influent the process.

5.2 Simulation configuration

The simulation is configured based on the initial condition of CCI-2 experiment. As shown in Figure 10, the corium and concrete are represented by blue and light blue particles. 3 layers virtual particles are placed outside of the concrete to keep the correct particle number density at the boundary area. The size of the melt pool is totally same as the initial condition of the experiment. However, because the melt didn't melt through neither basemat nor sidewall, thus the size of the concrete is cut to half compare to the real case to save the calculation time. The initial condition of the simulation is shown in Table 5.

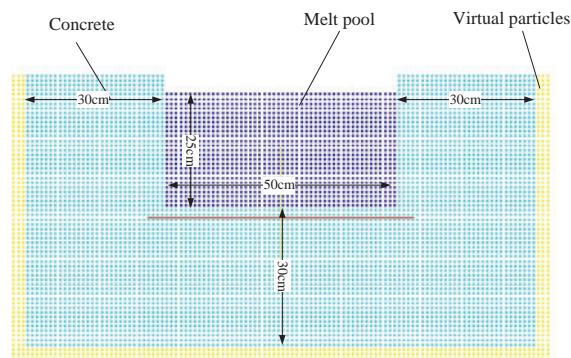


Figure 10. Initial configuration of the simulation

Table 5. Initial condition of the simulation

Parameter	Value
Initial temperature of Corium (K)	2153.0
Initial temperature of concrete (K)	293.0
Average distance between particles (m)	0.01
Total number of particles	6992
Input power(kW)	150kW

5.3 Result discussion

Figure 11 shows the comparison of the ablation depth between the experiment and the simulation. From the picture, we can see the ablation behavior is almost homogenous, which matches the experimental results. However, the slower ablation speed compare to the experiment can be seen. The possible reason is the thermal release from the oxidation heat is not considered in this simulation. Besides, an ablation jump can be observed around 50min in the basemat in Figure 11 because of the crust is broken and subsequently a lot of chemical reaction between the metallic and liquid concrete, while it didn't revealed in the simulation results because the heat released from the chemical reaction is not considered yet, which suggest the importance of chemical reaction and gas generation.

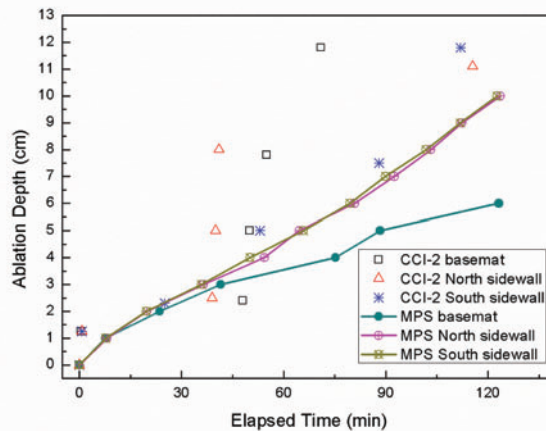


Figure 11. Initial configuration of the simulation

6 Conclusion

A new MPS code was developed aiming to simulate MCCI process. Heat transfer model, phase-change model, natural circulation model and mixing model were implemented in the code to emulate MCCI phenomena, and were validated against the experiments. Since the heat transfer and phase change are of importance for the MCCI analysis, that suggests these models might be able to extended to the real MCCI simulation.

1. Reasonable results can be obtained by simulating the experiment with melting tin [32]. The temperature distribution agrees with the experiment results. However, it also shows MPS method contribute the calculation deteriorate at the high Rayleigh Number conditions.
2. A small scale experiment was conducted using U-alloy and gel wax to emulate the ablation behavior in MCCI. The motion of the U-alloy melt was visualized and temperature history was measured as an experimental data for code validation.
3. The wax experiment was simulated using the developed MPS code, and the calculation results were compared. The ablation behavior, deformation profile of molten metal and temperature history matched the results of the experiment, which demonstrates the possibility of the MPS code's application for the simulation of the physical phenomena existing in an MCCI event.
4. CCI-2 experiment is simulated using the developed MPS code, and the calculation results were compared. As the major parameter of the experiment, the ablation rate and the melt temperature shows the similar trend. However, the difference can be seen from the comparison, which mainly because the chemical reaction and gas generation was not considered yet in this simulation.

Since the MCCI process is quite complicated, the calculation for CCI-2 experiment is separated from several steps. This paper shows the results of the first step. In the next step, the chemical reaction and gas generation will be considered in the simulation.

References

1. H. Alsmeyer et al, "Molten corium/concrete interaction and corium coolability - A state of the art report," European Commission Report EUR 16649, 1995.
2. D.H. Thompson, M.T. Farmer, J.K. Fink, D.R. Armstrong, B.W. Spencer, and Compilation, "analysis and interaction of ACE Phase C and MACE experimental data," Argonne National Laboratory, Chicago, IL, USA Report ACEX TRC-14, 1997.
3. E. R. Copus, "Sustained Uranium dioxide Concrete interaction tests: The SURC test series, 2nd OECD (NEA) Spec. Mtg. on Molten Core Debris/Concrete Interactions," Karlsruhe 1992.
4. D.H. Thompson, M.T. Farmer, J.K. Fink, D.R. Armstrong, B.W. Spencer, and Compilation, "Core-Concrete Interactions Using Molten Urania With Zirconium on a Limestone Concrete Basemat, The SURC-1 Experiment," Sandia National Lab 1992.
5. E. R. Copus, R. E. Blose, J. E. Brockmann, R. B. Simpson, and D. A. Lucero, "Core-Concrete Interactions using Molten UO₂ with Zirconium on a Basaltic Basemat: The SURC-2 Experiment," Sandia Nat. Lab, U.S. Report NUREG/CR-5564, 1990.
6. E. R. Copus, R. E. Blose, J. E. Brockmann, R. D. Gomez, and D. A. Lucero, "Core-Concrete Interactions using Molten Steel with Zirconium on a Basaltic Basemat: The SURC-4 Experiment," Sandia National Laboratories NUREG/CR-4994, 1989.
7. R. E. Blose, D. A. Powers, E. R. Copus, J. E. Brockmann, and R. B. Simpson, "Core- Concrete Interactions with Overlying Water Pools - The WETCOR-1 Test," Sandia Nat. Lab, U.S.A. Report NUREG/CR-5907, SAND92-1563, 1993.
8. M. T. Farmer, B. W. Spencer, D. J. Kilsdonk, and W. Aeschlimann, "Status of large scale MACE Core Coolability experiments, OECD Workshop on Ex-Vessel Debris Coolability," Karlsruhe, Germany 1999.
9. M.T. Farmer, S. Lomperske, and D.J. Kilsdonk, "OECD MCCI Project 2-D Core Concrete Interaction (CCI) Tests: Final Report," Argonne National Laboratory 2006.
10. M. T. Farmer, S. W. Lomperski, and S. Basu, "The Results of the CCI-3 Reactor Material Experiment Investigating 2-D Core-Concrete Interaction and Debris Coolability with a Siliceous Concrete Crucible," Advanced Nuclear Power Plants (ICAPP' 06), 2006.
11. Cranga, C. M.; Mun, B. Michel, F. Duval, and M. Barrachin, "Interpretation of real material 2D MCCI experiments in homogeneous oxidic pool with the ASTEC/MEDICIS code," Institut de Radioprotection et Surete Nucleaire, United States 2008.
12. M. Cranga, B. Spindler, E. Dufour, D. Dimov, K. Atkhen, J. Foit, *et al.*, "Simulation of corium concrete interaction in 2D geometry," *Progress in Nuclear Energy*, vol. 52, pp. 76-83, 1// 2010.
13. M. T. Farmer, "Modeling of ex-vessel corium coolability with the CORQUENCH code," Argonne National Lab, United States ANL/RAE/CP-103161, 2001.
14. e. a. J.J. Foit, "The wechsl-mod3 code : a computer program for the interaction of a core melt with concrete including the long term behavior model description and user's manual," Kernforschungszentrum Karlsruhe, Karlsruhe, Germany 1995.
15. V. Strizhov, V. Kanukova, T. Vinogradova, and E. Askenov, "An Assessment of the CORCON-MOD3 Code Part I: Thermal-Hydraulic Calculations," Russian Academy of Sciences NUREG/IA-0129, 1996.
16. T. SAKAI and H. GOTOH, "LAGRANGIAN SIMULATION OF BREAKING WAVES USING PARTICLE METHOD," *Coastal Engineering Journal*, vol. 41, pp. 303-326, 1999.
17. T. W. H. Sheu, C. Chiao, and C. Huang, "Development of a Particle Interaction Kernel Function in MPS Method for Simulating Incompressible Free Surface Flow," pp. 1-16, 2011 2011.
18. K. M. K. F. N. S. Shuai Zhang, "SIMULATION OF THE INCOMPRESSIBLE FLOWS WITH THE MPS METHOD " *13th International Conference on Nuclear Engineering* vol. 13-50166, May 16-20, 2005 2005.
19. H. Young Yoon, S. Koshizuka, and Y. Oka, "A particle-gridless hybrid method for incompressible flows," *International Journal for Numerical Methods in Fluids*, vol. 30, pp. 407-424, 1999.
20. S. Koshizuka and Y. Oka, "Moving-particle Semi-implicit Method for Fragmentation of Incompressible Fluid," *Nuclear Science and Engineering*, vol. 123, pp. 421-434, 1996.

21. S. Koshizuka, A. Nobe, and Y. Oka, "Numerical Analysis of Breaking Waves Using the Moving Particle Semi-implicit Method," *INTERNATIONAL JOURNAL FOR NUMERICAL METHODS IN FLUIDS*, vol. Meth. Fluids 26, pp. 751-769, 1998.
22. S.Koshizuka and Y.Oka, "Application of Moving Particle Semi-implicit Method To Nuclear Reactor Safety," *Advanced Methods for Computational Fluid Dynamics*, vol. 9, pp. 366-375, 2001.
23. X. Li and Y. Oka, "Numerical simulation of the SURC-2 and SURC-4 MCCI experiments by MPS method," *Annals of Nuclear Energy*, vol. 73, pp. 46-52, 11// 2014.
24. M. Kondo, S. Koshizuka, and M. Takimoto, "Surface tension model using inter-particle force in Particle method," presented at the 5th Joint ASME/JSME Fluids Engineering Conference, California USA, 2007.
25. M. Akgün, O. Aydın, and K. Kaygusuz, "Experimental study on melting/solidification characteristics of a paraffin as PCM," *Energy Conversion and Management*, vol. 48, pp. 669-678, 2// 2007.
26. N. Ukrainczyk, S. Kurajica, and J. Šipušić, "Thermophysical Comparison of Five Commercial Paraffin Waxes as Latent Heat Storage Materials," *Chemical & Biochemical Engineering Quarterly*, vol. 24, 2009.
27. L. Yuanyuan and C. Xiaoming, "Review on the low melting point alloys for thermal energy storage and heat transfer applications," *Energy Storage Science and Technology*, vol. 2, pp. 189-198, 2013.
28. V. Asmolov, N. N. Ponomarev-Stepnoy, V. Strizhov, and B. R. Sehgal, "Challenges left in the area of in-vessel melt retention," *Nuclear Engineering and Design*, vol. 209, pp. 87-96, 11// 2001.
29. T. G. Theofanous, M. Maguire, S. Angelini, and T. Salmassi, "The first results from the ACOPO experiment," *Nuclear Engineering and Design*, vol. 169, pp. 49-57, 6/1/ 1997.
30. J.M.Bonnet and J.M.Seiler, "Thermal Hydraulic Phenomena In Corium Pools: The BALI Experiment," in *7th International Conference on Nuclear Engineering*, Tokyo, Japan, 1999.
31. J. Lewins and M. Becker, *Advances in Nuclear Science & Technology*, 1999.
32. F. Wolff, C. Beckermann, and R. Viskanta, "Natural convection of liquid metals in vertical cavities," *Experimental Thermal and Fluid Science*, vol. 1, pp. 83-91, 1// 1988.
33. M. T. Farmer, S. Lomperski, D. J. Kilsdonk, R. W. Aeschlimann, and S. Basu, "OECD/MCCI 2-D Core Concrete Interaction (CCI) tests : final report February 28, 2006," OECD/MCCI-2005-TR05; TRN: US1102884 United States 10.2172/1014855 TRN: US1102884 Thu Jun 23 07:34:53 EDT 2011 AN ENGLISH, 2011.